A 2.7 to 9.3 GHz CMOS Wideband Amplifier Combined with High Pass Filter for UWB system

Mun-Sook Jung, Chang-Wan Kim, Phan Tuan Anh, Hoon-Tae Kim[1] and Sang-Gug Lee

Information and Communications University, Daejeon, Korea

[1]Samsung Advanced Institute of Technology, Suwon, Korea

Abstracts - A new wideband amplifier, which is suitable for Ultra-wideband (UWB) system, is proposed in this paper. The proposed amplifier achieves wideband input matching and bell-shaped overall frequency response by combining the frequency response characteristics of a high pass filter and a conventional amplifier, respectively. The simulation results based on a TSMC 0.18 μm CMOS technology show a peak power gain of 10 dB, input return loss (S_{11}) of larger then 10 dB over the -3 dB bandwidth from 2.7 to 9.3 GHz, and minimum noise figure of 3.3 dB in pass-band. The wideband amplifier dissipates 7 mA from a 2 V supply.

Keywords – wideband amplifier, CMOS, LNA, RFIC UWB, ultra-wideband

1. Introduction

In recent years, ultra-wideband system has emerged as a prominent technology in wireless communication systems. The application of UWB technology is expected to imaging system, ground penetrating radars, and wireless home network, etc.. For the wireless home network application, the unlicensed UWB frequency band is allocated from 3.1 to 10.6 GHz [1] and it can provide higher data-rate with its wide bandwidth than that of other current wireless communications systems. However, all circuits for UWB system should have wideband characteristics. Especially, the wideband amplifier for the UWB system is required to have wideband input matching and wide bandwidth. In addition, the frequency response shape of the amplifier is recommended to have bell-shaped like a band pass filter to suppress strong interferers.

Recently, there are numbers of reported UWB low noise amplifiers (LNA) adopting a 3rd–section passive band pass filter (BPF) at the input node of the amplifier to achieve wideband input matching and wide bandwidth, which have the shape of frequency response like that of band pass filter [2], [3]. However, they use many passive reactive components at the input stage of the amplifier, leading to larger chip area and degradation of noise performance due to parasitic components.

In this paper, the proposed wideband amplifier combines the frequency response characteristic of a high pass filter (HPF) with that of a conventional amplifier to achieve wideband input matching and wide bandwidth.

2. Design of amplifier

Fig. 1 shows the combination of frequency response of high pass filter and low pass filer (LPF) achieve that of band pass filter in linear system. As shown in Fig. 1, the upper and lower –3 dB cut-off frequency (ω_H and ω_L) of the BPF can be decided by the –3 dB cut-off frequency of LPF and HPF, respectively.

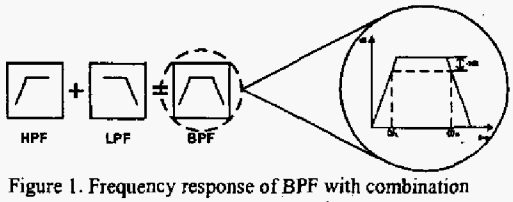

Figure 1. Frequency response of BPF with combination of that of HPF and LPF, respectively.

In Fig. 1, the LPF can be replaced with a general resistively loaded amplifier, which inherently shows low pass response characteristic with some passband voltage gain. From this simple concept, an amplifier with band pass characteristics can be implemented.

Fig. 2 shows the proposed wideband amplifier combined with a HPF. As can be seen in Fig. 2, a HPF is embedded into the input of the cascode amplifier. The adoption of HPF instead of BPF can reduce noise figure of overall amplifier because the number of passive component at the input gate of amplifier decreases. In Fig. 2, HPF is consisted of C_1, L_1, and C_2 (C_{ext} and C_{GS1}) and the cascode amplifier M_1 and M_2 adopts the shunt-peaking load (L_L and R_L). The wideband buffer (M_3) is used for the wideband output matching.

In general, HPF can be designed with T type or Π type [4]. In Fig. 2, a T type HPF is chosen to reduce the number of inductors and simplify the bias circuit of the cascode amplifier. In addition, to achieve high attenuation characteristics for out of band, a Chebyshev 3rd-section method is adopted in this work. In Fig. 2, the –3 dB cut-off frequency is given by:

$$\omega_L = 1/(2\sqrt{L_1 C_1}). \quad (1)$$

Initially, HPF is connected into the input of an amplifier, the values of passive components are selected as C_1 = 1 pF, L_1 = 2.6 nH, and C_2 = 1 pF, respectively. From these values, simulation results for the HPF show input resonance frequency of 4 GHz and attenuation of -10 dB at 1.7 GHz. In addition, the -3 dB cut-off frequency of HPF is decided at 2.3 GHz. When the HPF is finally combined into the input of the amplifier, the value of C_2 is optimized as 0.4 pF.

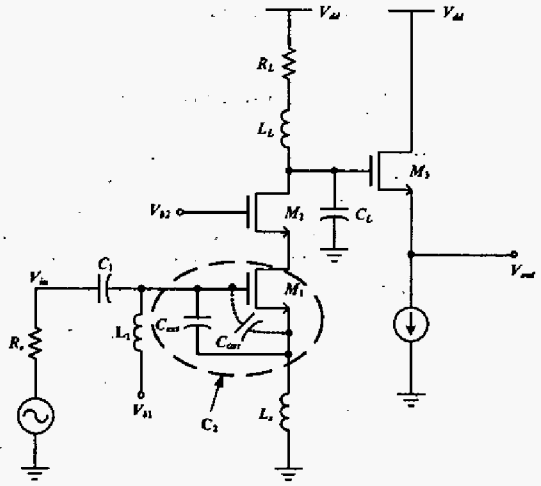

Figure 2. Proposed wideband amplifier.

In Fig. 2, the cascode amplifier inherently shows low pass frequency response characteristic due to its dominant pole at the drain node of M_2. The dominant pole of amplifier is given by:

$$\omega_{-3dB} = 1/(R_L C_L). \quad (2)$$

Where R_L is resistive load and C_L total parasitic capacitances at the drain node of M_2. From (2), to control the -3 dB cut-off frequency of the cascode amplifier, R_L or C_L can be changed. Because the total parasitic capacitances C_L is difficult to control, R_L can be more easily used to control the bandwidth. In Fig. 2, the -3 dB bandwidth of the amplifier is decided at 9.5 GHz with R_L = 90 Ω and L_L = 2.6 nH, considering reasonable gain and noise characteristics. In Fig. 2, the shunt-peaking inductor L_L is used as an additional control parameter, which can improve the 3-dB bandwidth without any additional dc power consumption [5]. In Fig. 2, source degeneration inductor L_S is adopted to generate real term (50 Ω) for improving the power matching between HPF and amplifier. In Fig. 2, C_{ext} is connected between the gate and source node of M_1 to reduce the size of input transistor M_1, leading to less dc power consumption under the same value of gate-source voltage of M_1 (V_{GS1}) [6]. Gain and noise figure of overall amplifier, however, are not affected. Moreover, the smaller size of transistor reduces parasitic capacitances at drain node of transistors, so that it can help to extend the -3 dB bandwidth. In Fig. 2, the value of C_{ext} is 350 fF.

From the simulation, voltage gain of the amplifier shows 10 dB in the pass-band. The input resonant circuit of the amplifier in Fig. 2, which includes C_{ext}, C_{GS1}, and L_S, resonates at 9 GHz.

Other design parameters in Fig. 2 are M_1 = 240/0.18 μm, M_2 = 80 /0.18 μm, and L_S = 0.9 nH, respectively.

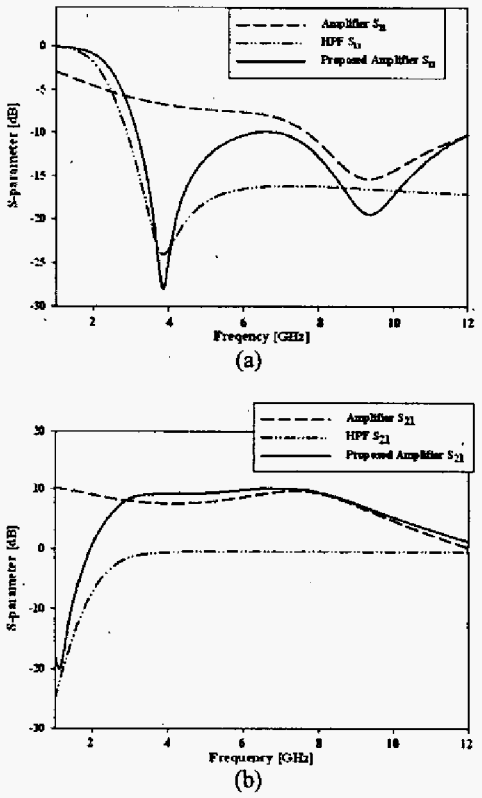

Figure 3. Simulated of S_{11} and S_{21} for HPF, the cascode amplifier, and the cascode amplifier combined with HPF, respectively: (a) input return loss (S_{11}) and (b) frequency response characteristics (S_{21})

Fig. 3-(a) and (b) show the simulated S_{11} and S_{21} for HPF, the cascode amplifier and the cascode amplifier combined with HPF, respectively. In Fig. 3-(a), the S_{11} of HPF and the cascode amplifier resonate at 4 and 9 GHz, respectively, so that the input return loss of overall amplifier combined with HPF in Fig. 3-(a) can be achieved larger than 10 dB over 3.1 ~ 12.9 GHz. In this way, wideband input matching can be achieved over interested frequency band by controlling each input resonance frequency of HPF and amplifier, respectively.

In Fig. 3-(b), the simulated S_{21} of HPF shows the conventional high pass frequency response with insertion loss of 0.4 dB and the -3 dB cut-off frequency of 2.3 GHz. The S_{21} trace of the cascode amplifier shows inherent low pass frequency response with gain of 9.8 dB and the -3 dB cut-off frequency of 9.5 GHz. The combined S_{21} of the cascode amplifier with HPF clearly shows overall bell-shaped band-pass frequency response over 2.7 ~ 9.3 GHz. Fig. 4 shows the simulation result of the proposed amplifier's noise figure. The minimum value of NF is 3.3 dB at 3.6 GHz and maximum value of 5.9 dB at 10.6 GHz in pass band. Fig. 5 shows the simulated input-referred IP3 of - 0.3 dBm in the proposed amplifier. The two-tone test is performed at 4 and 4.5 GHz. Fig. 6 shows layout photograph of the proposed amplifier.

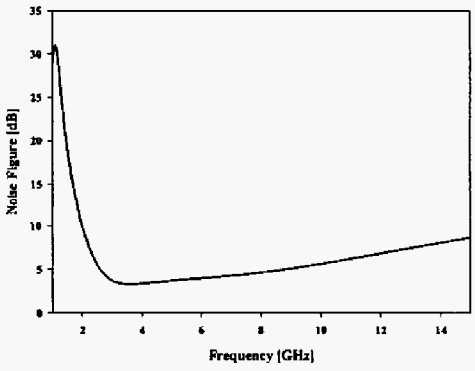

Figure 4. Simulated noise figure of the proposed amplifier.

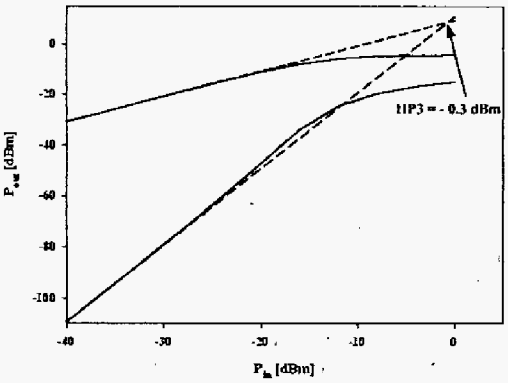

Figure 5. Simulated two-tone test of the proposed amplifier.

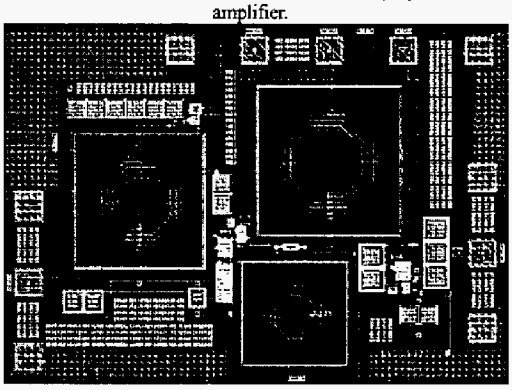

Figure 6. Layout (1,000 μm x 800 μm).

3. SUMMARY

The new wideband amplifier, which combines a 3rd-section HPF with a cascode amplifier, is presented and the design concept is also discussed. The proposed amplifier can achieve wideband input matching and bell-shaped overall frequency response over UWB frequency band. The simulation results based on a TSMC 0.18 μm CMOS technology show the -3 dB bandwidth of 2.7 ~ 9.3 GHz, return loss (S_{11}) of greater than 10 dB over 3.1 ~ 12.9 GHz, peak power gain of 10 dB, and minimum noise figure of 3.3 dB in pass-band, while consuming only 7 mA from a 2 V supply.

REFERENCES

[1] http://www.ieee802.org/15/pub/TG3a.html

[2] Andrea Bevilacqua, Ali M Niknejad, "An Ultra-wideband CMOS LNA for 3.1 to 10.6 GHz Wireless Receivers," *IEEE Solid State Circuits conf.*, pp. 382-383, February 2004.

[3] A. Ismail, A. Abidi, "A 3 to 10 GHz LNA Using a

Wideband LC-ladder Matching Network," *IEEE Solid State Circuits conf.*, pp. 384-385, February 2004.
[4] Jia-Sheng Hoang and M.J.Lancaster, Microstrip Filter for RF/Microwave Applicatons.
[5] Sunderaerjan S. Mohan, Maria del Mar Hershenson, Stephen P. Boyd, and Thomas H. Lee, "Bandwidth Extension in CMOS with Optimized On-Chip Inductors," *IEEE J. Solid State Circuits*, vol. 35, NO. 3, pp. 346-355, March. 2000.
[6] Trung-Kien Nguyen, Chung-Hwan Kim, Gook-Ju Ihm, Moon-Su Yang, and Sang-Gug Lee. "CMOS Low Noise Amplifier Design Optimization Techniques," *IEEE Trans. Microwave Theory Tech.*, vol. 52, NO. 5, pp. 1433-1442, May 2004.